Designing future
CMB experiments

Peering at the CMB through the polarized Galaxy

Jacques Delabrouille

CNRS, laboratoire APC

and

CEA, Département d'Astrophysique

Outline

- Astrophysical foreground emission
- Basics of foreground cleaning
- Component separation methods
- Forecasting and validation
- Summary

Planck maps at 9 different frequencies

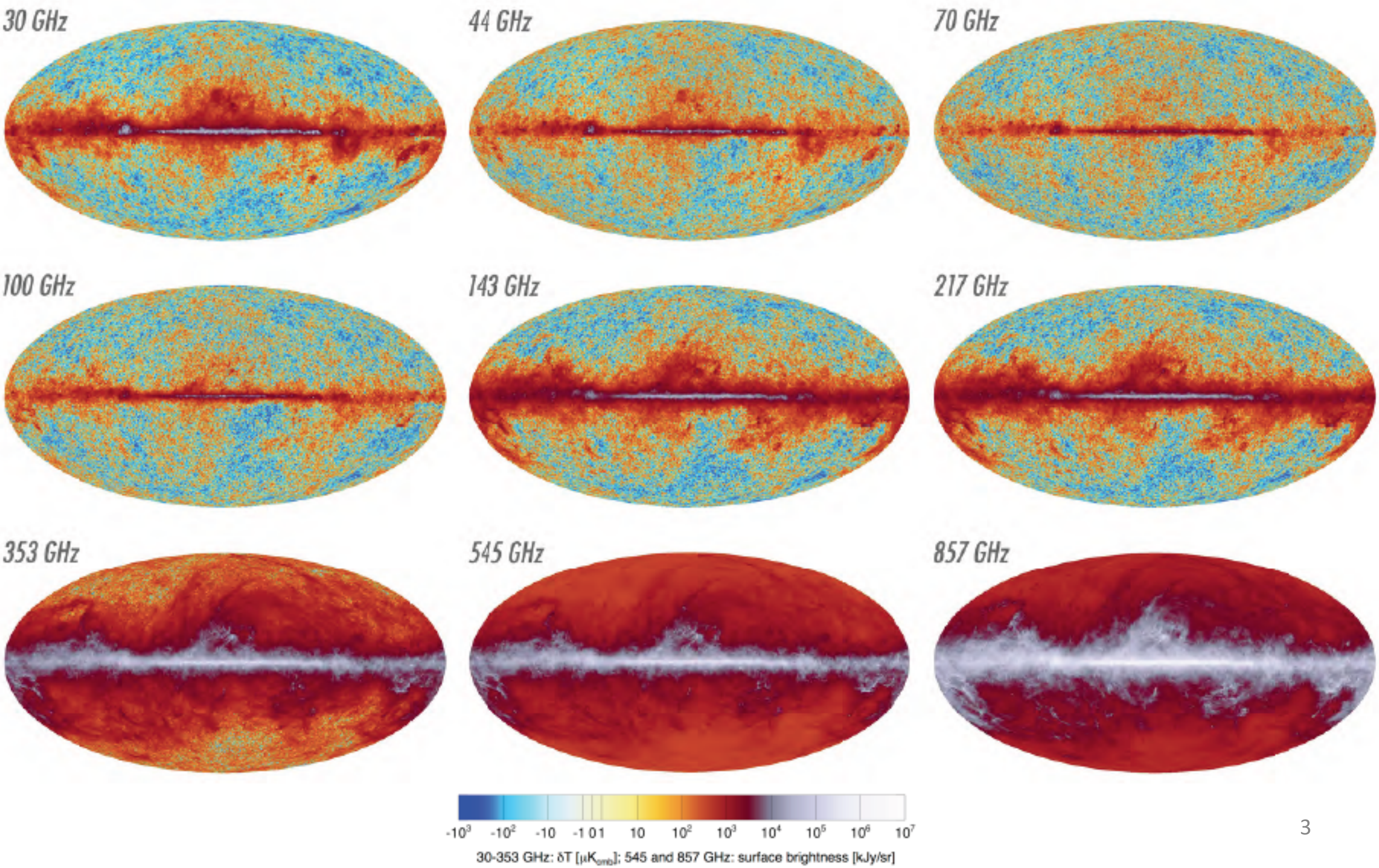

Planck polarisation maps (7 frequencies)

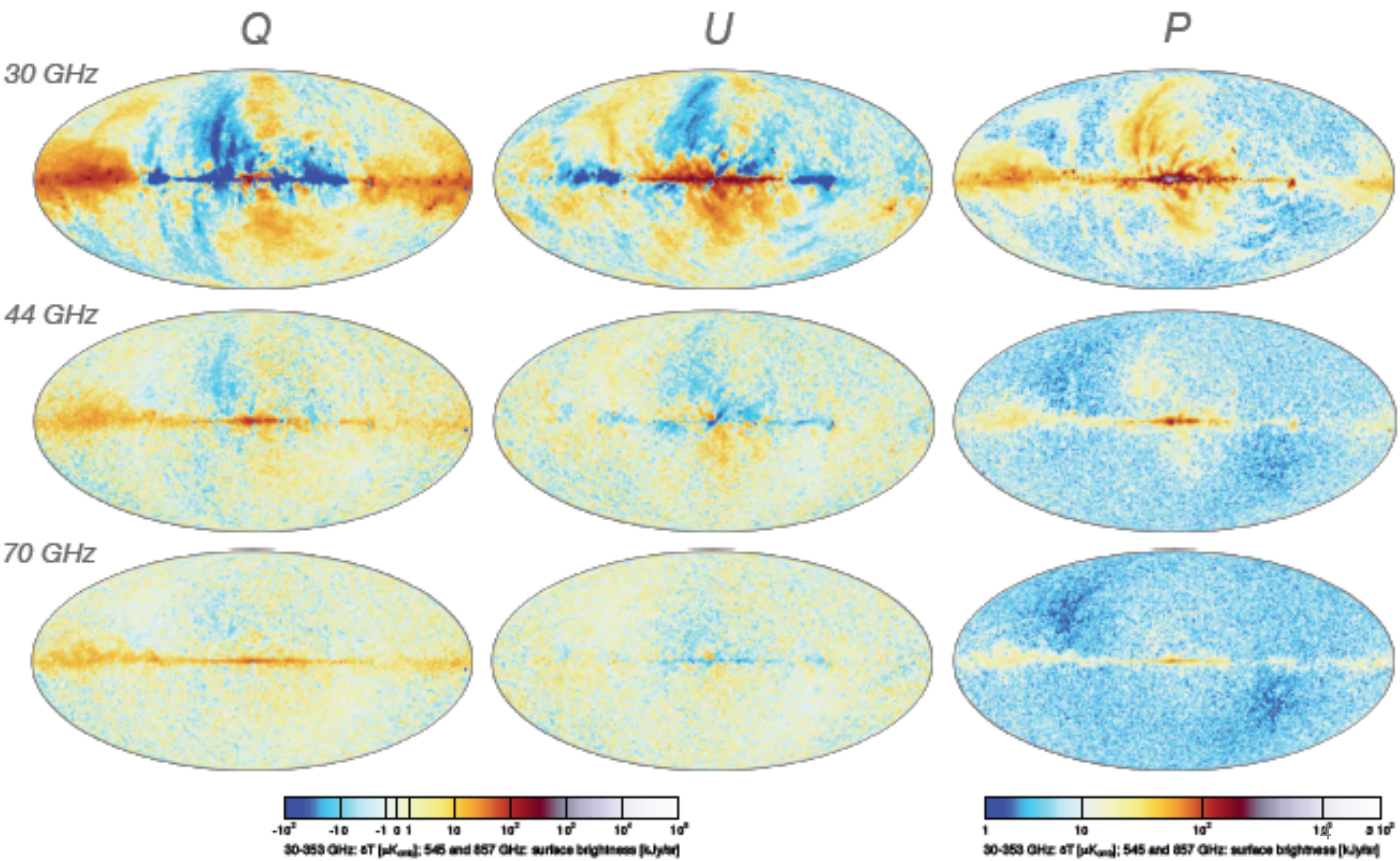

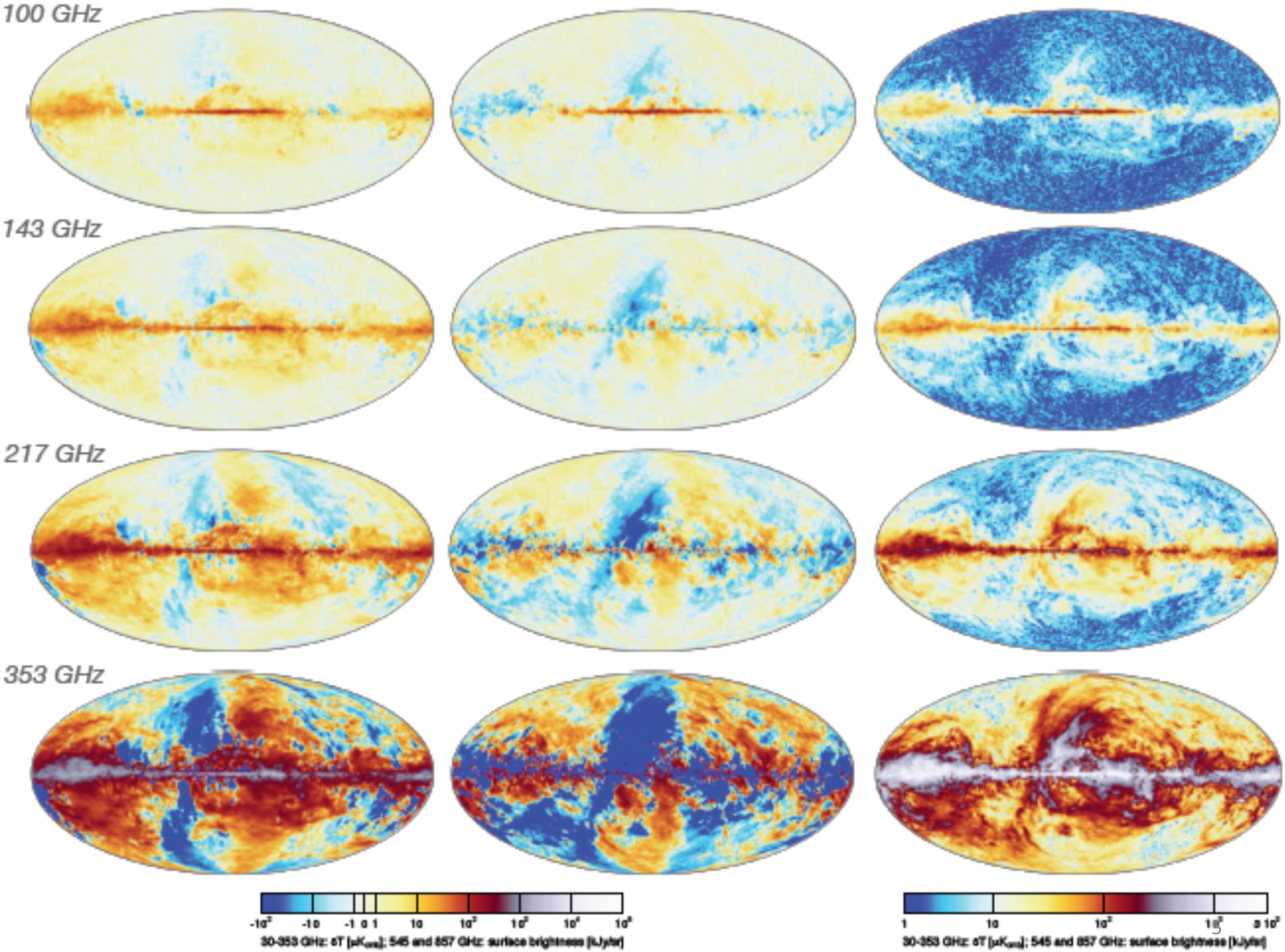

100 GHz
143 GHz
217 GHz
353 GHz
30-353 GHz: δT [μK_CMB]; 545 and 857 GHz: surface brightness [kJy/sr]
30-353 GHz: δT [μK_CMB]; 545 and 857 GHz: surface brightness [kJy/sr]

Foreground astrophysical emission

- Interstellar Medium (ISM)
  - Cosmic rays
  - Gas (ionised, neutral atoms, molecules, …)
  - Dust (macro-molecules, grains of matter of various size and composition)
  - Magnetic field

- The galactic ISM emits radiation through various processes
  - Synchrotron: cosmic rays in magnetic field
  - Free-free: ionised gas
  - Spectral lines: rotation and vibration of molecules, desexcitation of atoms
  - Thermal emission: from dust matter particles heated by stellar light
  - Electric emission from rotating dipoles
  - …

- There also are extragalactic sources of foreground emission (galaxies; clusters of galaxies: Sunyaev Zel'dovich – or SZ – effect)

Polarised galactic emission

- Synchrotron and thermal dust emissions are the dominating astrophysical foreground emissions.

- Both synchrotron and dust are polarised

Synchrotron

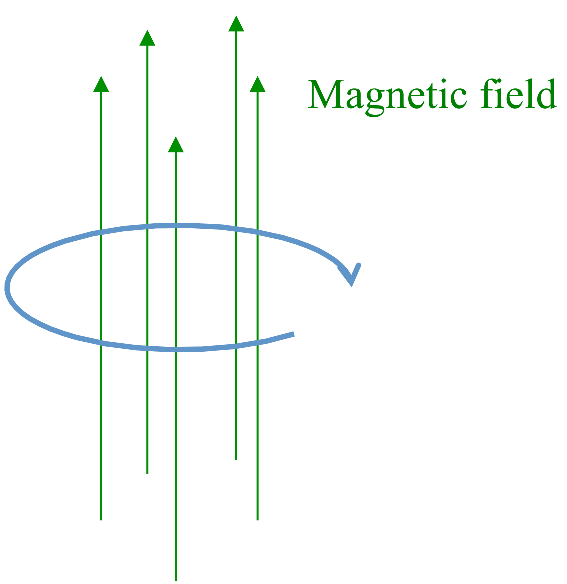

Dust

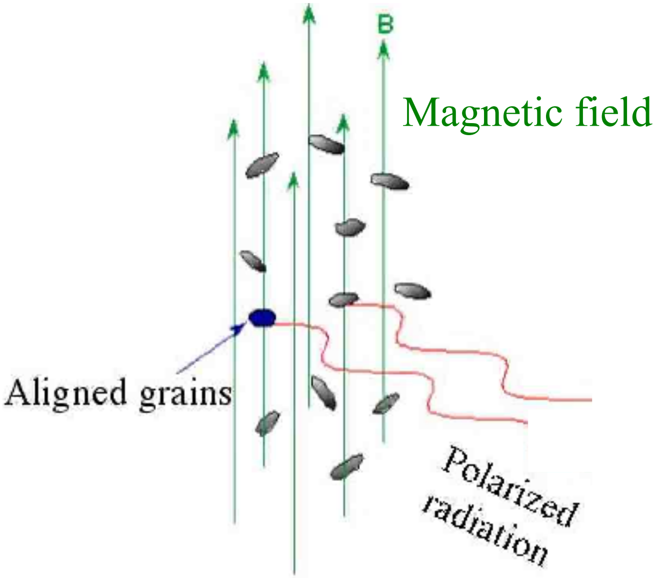

Elongated dust grains: projection effects

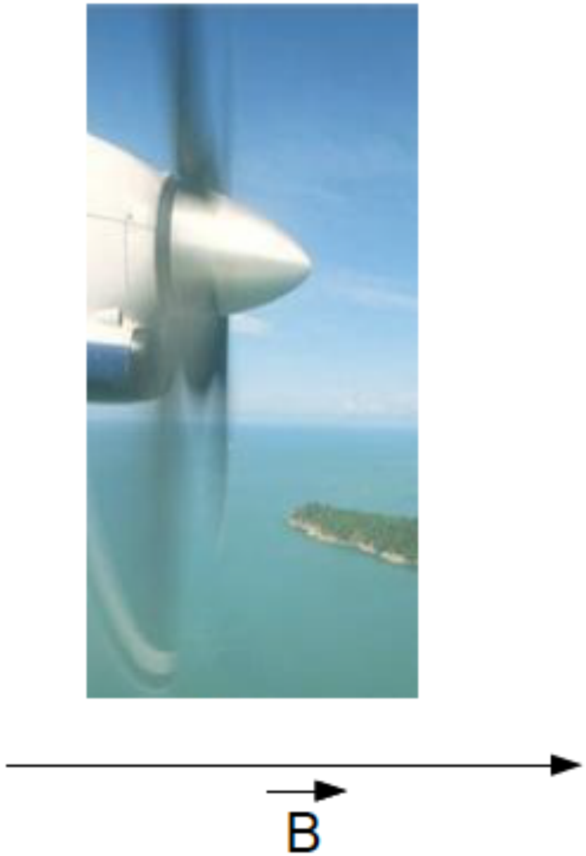

Polarization is maximal

Polarization is zero

From Vincent Guillet

Amplitude relative to CMB polarisation

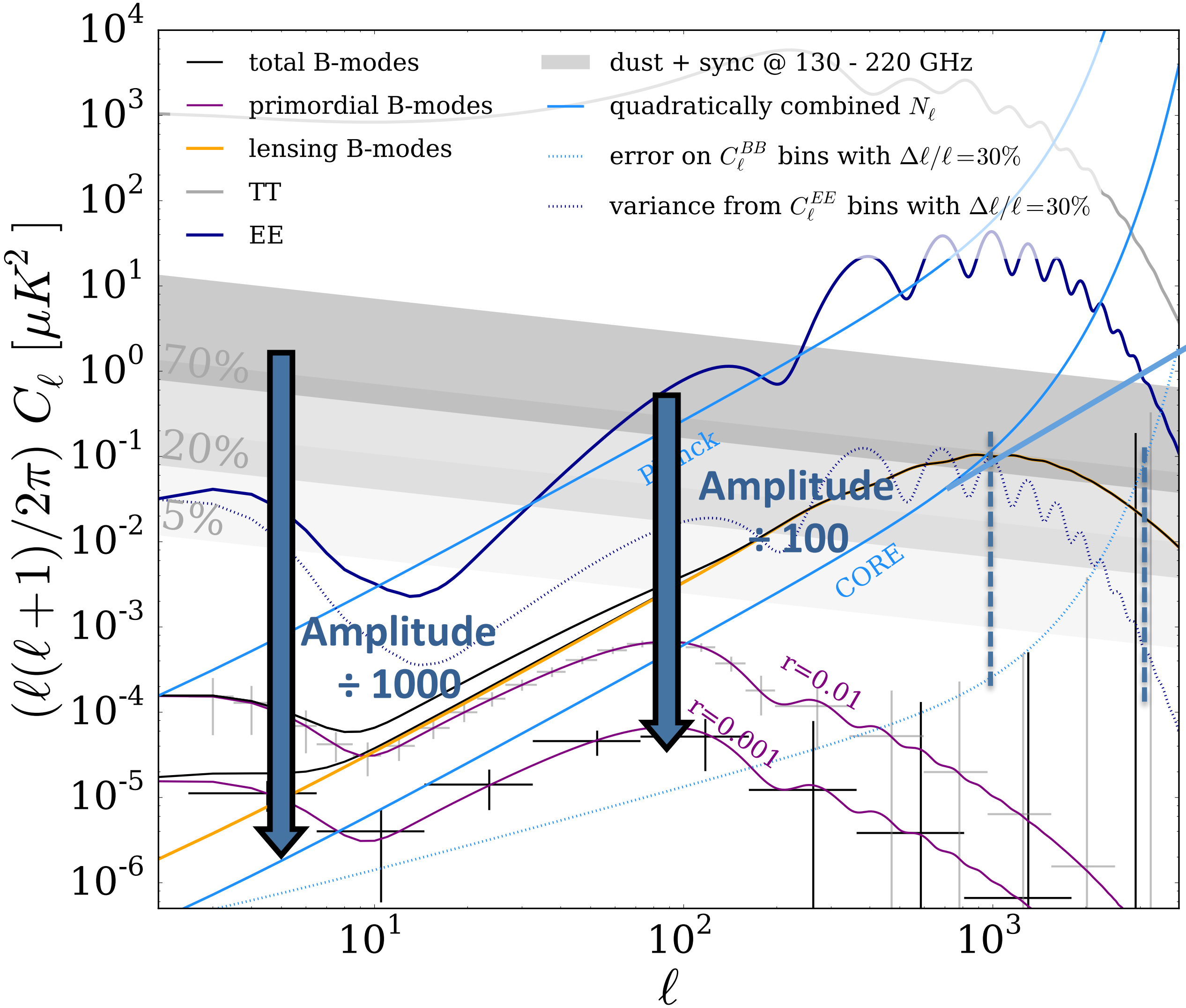

CORE
≈ 2 μK.arcmin

Foregrounds
70% sky
20% sky
5% sky

Outline

Astrophysical foreground emission

→ Basics of foreground cleaning

Component separation methods

Forecasting and validation

Summary

Foregrounds seen by Planck

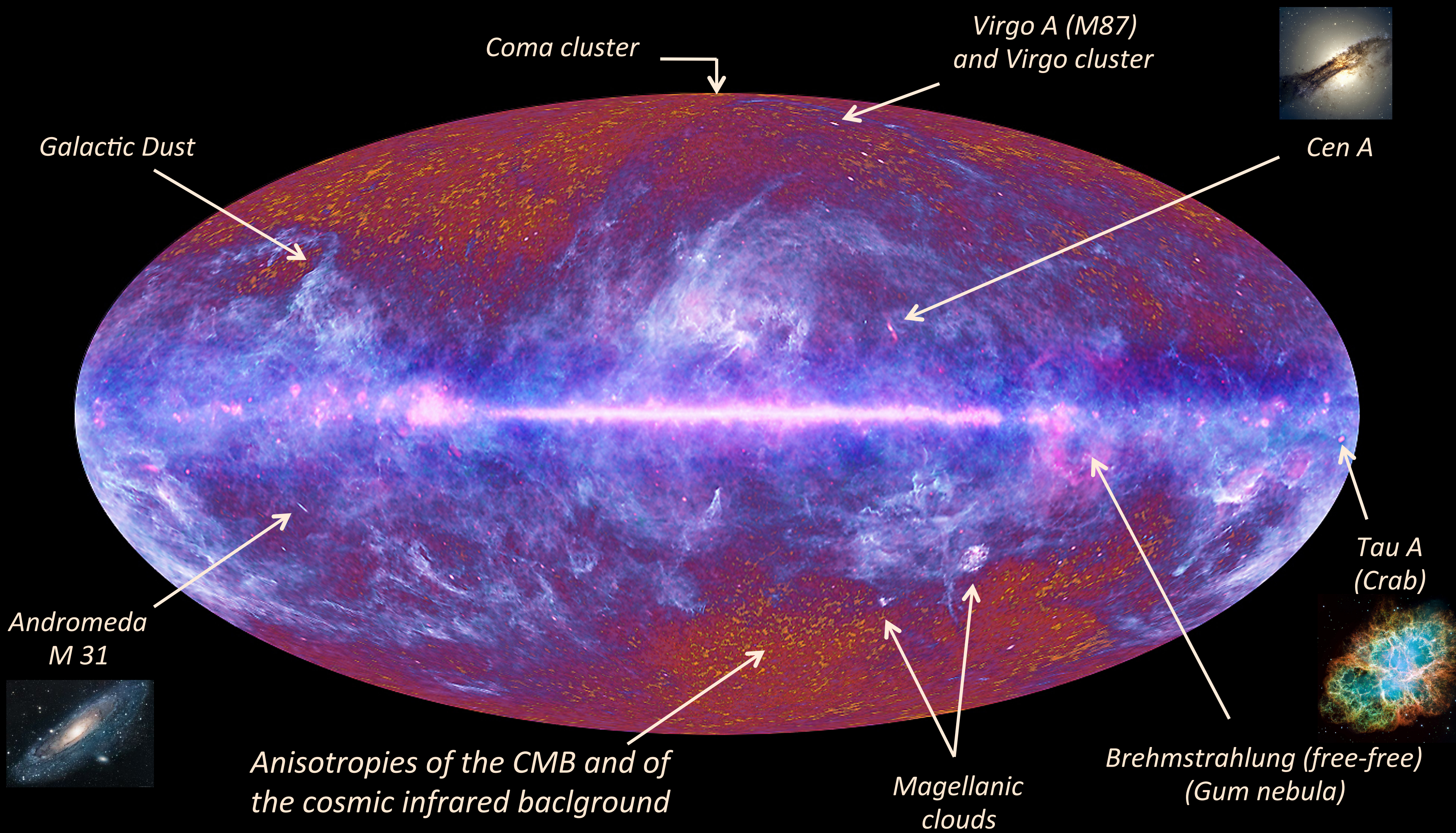

Relative amplitudes depend on frequency

Synchrotron is redder than the CMB (dominates at low frequency)
Dust is bluer than the CMB (dominates at high frequency)

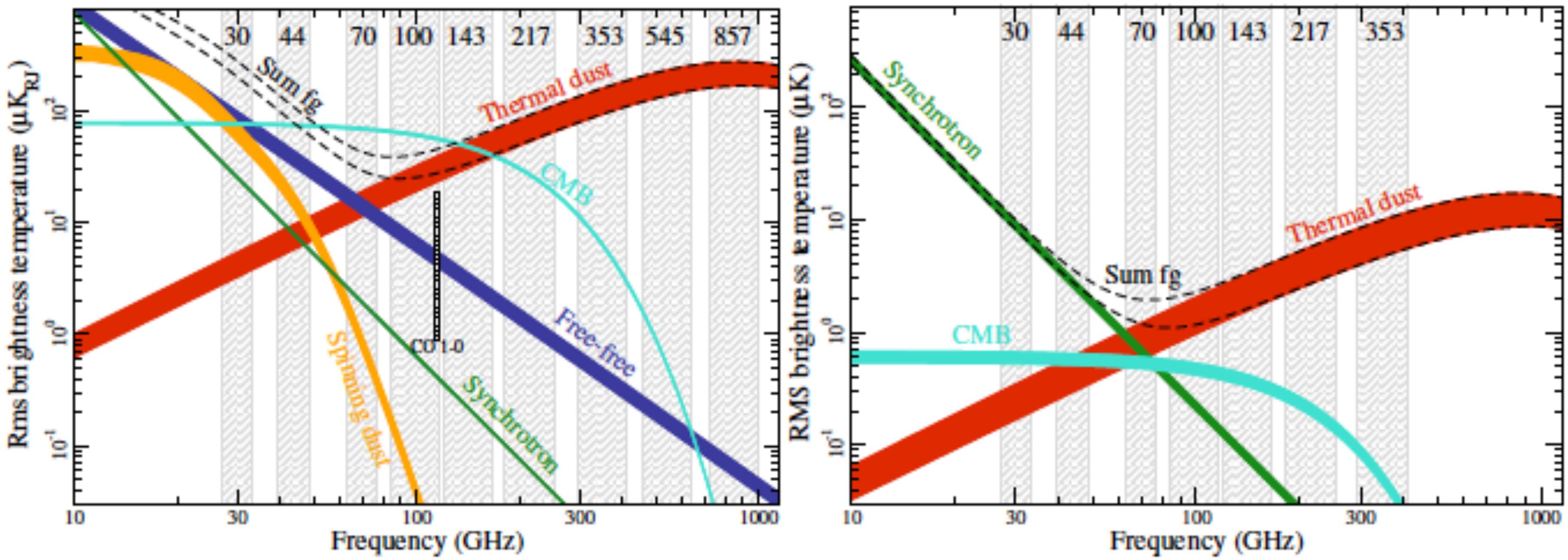

Fig. 18. Brightness temperature rms of the high-latitude sky as a function of frequency and astrophysical component for temperature (*left*) and polarization (*right*). For temperature, each component is smoothed to an angular resolution of 1° FWHM, and the lower and upper edges of each line are defined by masks covering 81 and 93 % of the sky, respectively. For polarization, the corresponding smoothing scale is 40′, and the sky fractions are 73 and 93 %.

Basics of foreground separation

Consider a single pixel p. The signal observed at frequency ν, in pixel p, is

$$x(\nu, p) = \sum_i x_i(\nu, p) + n(\nu, p)$$
$$= \sum_i a_i(\nu, p)\, s_i(p) + n(\nu, p),$$

or, in vector-matrix format

$$\boldsymbol{x}(p) = \mathrm{A}(p)\, \boldsymbol{s}(p) + \boldsymbol{n}(p).$$

Model known *a priori* ?
$dB_\nu/dT.s_{CMB} + s_{dust}.\nu^{\beta}B_\nu(T_d) + s_{sync}.\nu^{\alpha}$

At some frequency ν_0

Noiseless linear inversion

$$\mathbf{x}(p) = \mathbf{A}\mathbf{s}(p)$$

If A is square (as many observations as components)

$$\widehat{\mathbf{s}}(p) = \mathbf{A}^{-1}\mathbf{x}(p)$$

If not (more observations than components)

$$\widehat{\mathbf{s}}(p) = \left[\mathbf{A}^T\mathbf{A}\right]^{-1}\mathbf{A}^T\mathbf{x}(p)$$

Noisy linear inversion

$$\mathbf{x}(p) = \mathbf{A}\mathbf{s}(p) + \mathbf{n}(p)$$

Still OK...: $$\widehat{\mathbf{s}}(p) = \left[\mathbf{A}^T\mathbf{A}\right]^{-1}\mathbf{A}^T\mathbf{x}(p)$$

Noisy linear inversion

$$\mathbf{x}(p) = \mathbf{A}\mathbf{s}(p) + \mathbf{n}(p)$$

Still OK…: $\widehat{\mathbf{s}}(p) = \left[\mathbf{A}^T\mathbf{A}\right]^{-1}\mathbf{A}^T\mathbf{x}(p)$

Noise covariance matrix $\mathbf{R}_n = \langle \mathbf{n}\mathbf{n}^T \rangle$

$$\widehat{\mathbf{s}}(p) = \left[\mathbf{A}^T\mathbf{R}_n^{-1}\mathbf{A}\right]^{-1}\mathbf{A}^T\mathbf{R}_n^{-1}\mathbf{x}(p)$$

CMBists' jargon:
"*Optimal*" or "*Generalized Least Square*" (GLS) inversion

Summary of linear inversion options

If A is square and invertible

$$\widehat{\mathbf{s}}(p) = \mathbf{A}^{-1}\mathbf{x}(p)$$

Need to know A

Generalisation for more observations than components

$$\widehat{\mathbf{s}}(p) = \left[\mathbf{A}^T\mathbf{A}\right]^{-1}\mathbf{A}^T\mathbf{x}(p)$$

Need to know A

Noise-weighted version

$$\widehat{\mathbf{s}}(p) = \left[\mathbf{A}^T\mathbf{R}_n^{-1}\mathbf{A}\right]^{-1}\mathbf{A}^T\mathbf{R}_n^{-1}\mathbf{x}(p)$$

Need to know A, R_n

Outline

Astrophysical foreground emission

Basics of foreground cleaning

→ Component separation methods

Forecasting and validation

Summary

What if unknown emission laws ?

- Assume a linear mixture of components for which we do not know the emission laws

$$\boldsymbol{x}(p) = A(p)\,\boldsymbol{s}(p) + \boldsymbol{n}(p)$$

Observed

Unknown emission laws

Unknown component ampltude

Noise

Parametric fitting

$$x(\nu) = s_{\rm c} + s_{\rm d}\left[\frac{\nu}{\nu_{\rm ref}}\right]^{\beta_d} B_\nu(T_d) + s_{\rm s}\left[\frac{\nu}{\nu_{\rm ref}}\right]^{\alpha_s} + n(\nu)$$

6 unknowns here: amplitudes of components $s_{\rm c}, s_{\rm d}, s_{\rm s}$

parameters of frequency scaling β_d, T_d, α_s

With enough frequencies of observation (here, more than 6), one can fit for both the parameters of frequency scaling and the amplitudes of components

Synchrotron and dust polarisation maps

30 GHz

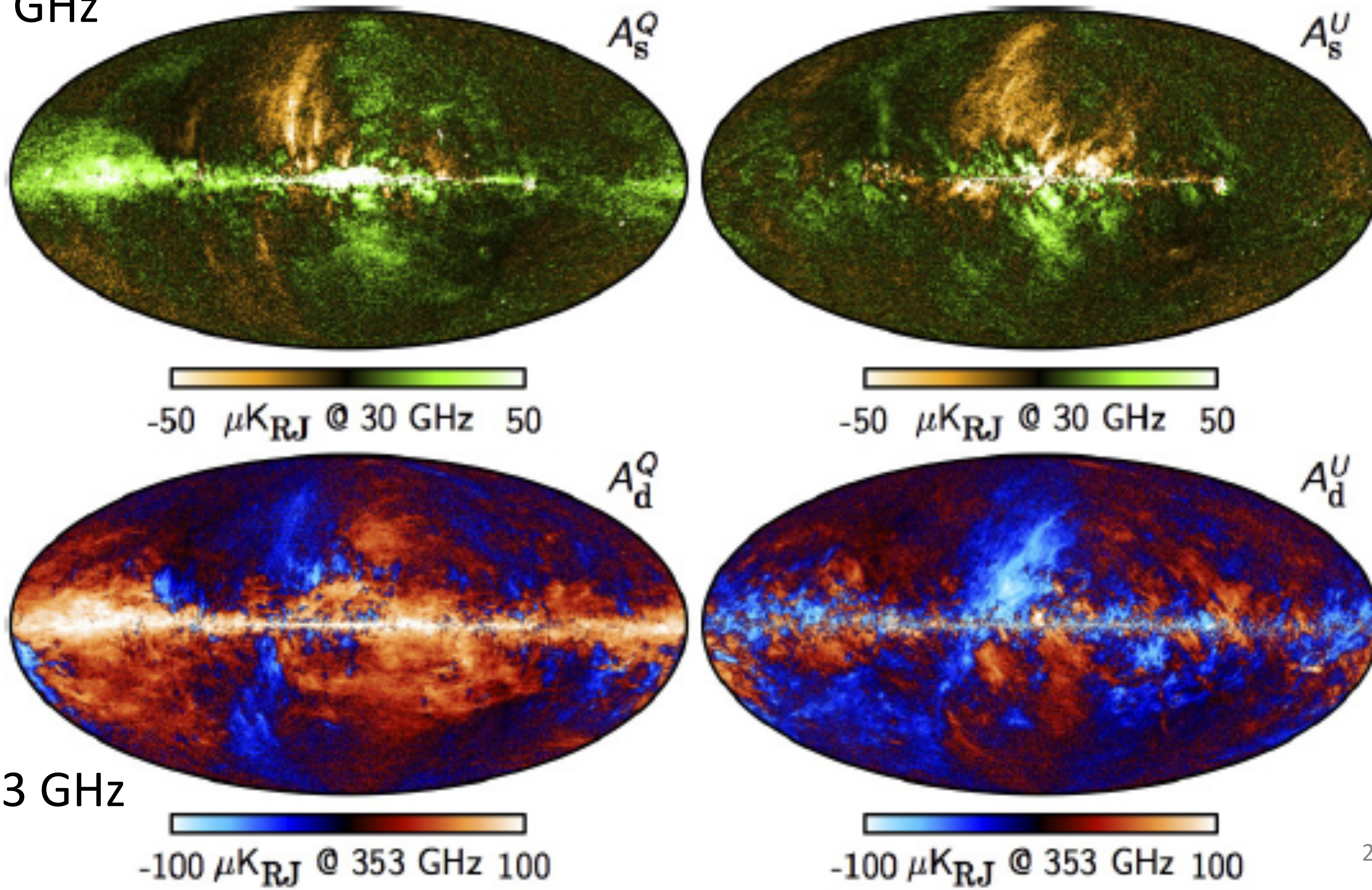

353 GHz

Key ingredients for it to work ?

- A trustable model for foreground emission laws
- Many frequency channels (more than parameters)

"Internal Linear Combination"

- What if we know only the emission law of one component of interest?

$$\mathbf{x}(p) = \mathbf{a}s(p) + \mathbf{n}(p)$$

One component of interest (usually the CMB)

Everything else is dumped in the noise term

"Internal Linear Combination"

$$\mathbf{x}(p) = \mathbf{a}s(p) + \mathbf{n}(p) \qquad \widehat{s}(p) = \frac{\mathbf{a}^t\mathbf{R}_n^{-1}}{\mathbf{a}^t\mathbf{R}_n^{-1}\mathbf{a}}\mathbf{x}(p)$$

- The "noise" covariance matrix is not known a priori
- But…

$$\begin{aligned}\mathbf{R}_x^{-1} &= \left[\mathbf{a}\mathbf{a}^t\sigma^2_{\mathrm{cmb}} + \mathbf{R}_n\right]^{-1} \\ &= \mathbf{R}_n^{-1} - \sigma^2_{\mathrm{cmb}}\frac{\mathbf{R}_n^{-1}\mathbf{a}\mathbf{a}^t\mathbf{R}_n^{-1}}{1+\sigma^2_{\mathrm{cmb}}\mathbf{a}^t\mathbf{R}_n^{-1}\mathbf{a}}\end{aligned}$$

- And hence

$$\begin{aligned}\mathbf{a}^t\mathbf{R}_x^{-1} &= \mathbf{a}^t\mathbf{R}_n^{-1} - \sigma^2_{\mathrm{cmb}}\frac{\mathbf{a}^t\mathbf{R}_n^{-1}\mathbf{a}\,\mathbf{a}^t\mathbf{R}_n^{-1}}{1+\sigma^2_{\mathrm{cmb}}\mathbf{a}^t\mathbf{R}_n^{-1}\mathbf{a}} \\ \mathbf{a}^t\mathbf{R}_x^{-1} &\propto \mathbf{a}^t\mathbf{R}_n^{-1}\end{aligned}$$

"Internal Linear Combination"

$$\widehat{s}(p) = \frac{\mathbf{a}^t \mathbf{R}_n^{-1}}{\mathbf{a}^t \mathbf{R}_n^{-1} \mathbf{a}} \mathbf{x}(p) = \frac{\mathbf{a}^t \mathbf{R}_x^{-1}}{\mathbf{a}^t \mathbf{R}_x^{-1} \mathbf{a}} \mathbf{x}(p)$$

- Actual implementation $$\widehat{s}_{\mathrm{ILC}}(p) = \frac{\mathbf{a}^t \widehat{\mathbf{R}}_x^{-1}}{\mathbf{a}^t \widehat{\mathbf{R}}_x^{-1} \mathbf{a}} \mathbf{x}(p)$$
  - Uses the empirical covariance matrix of the observations (and this is a very important distinction)

- Usually derived as the (internal) linear combination of the input maps which minimizes the variance of the output, with unit response to the CMB

$$\widehat{s}_{\mathrm{ILC}}(p) = \sum_i w_i x_i(p) = \mathbf{w}^t \mathbf{x}(p)$$

$$\sum_i w_i a_i = \mathbf{w}^t \mathbf{a} = 1$$

$$\text{minimize } \sum_p |\widehat{s}(p)|^2$$

"Internal Linear Combination"

Around *l,b = (70°,-30°)* – Moderate galactic latitudes

Original map

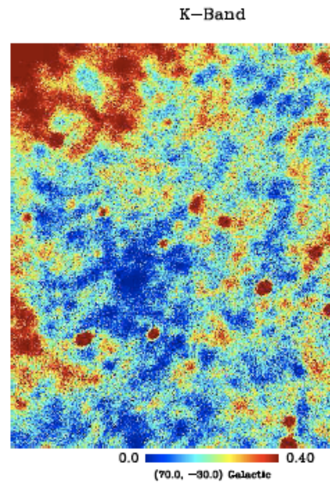

WMAP K band at 23 GHz dominated by galactic synchrotron

In a given pixel:

- CMB?
- galactic ISM?
- radio source ?

"Internal Linear Combination" results

Original map

Estimated CMB

CMB subtraction

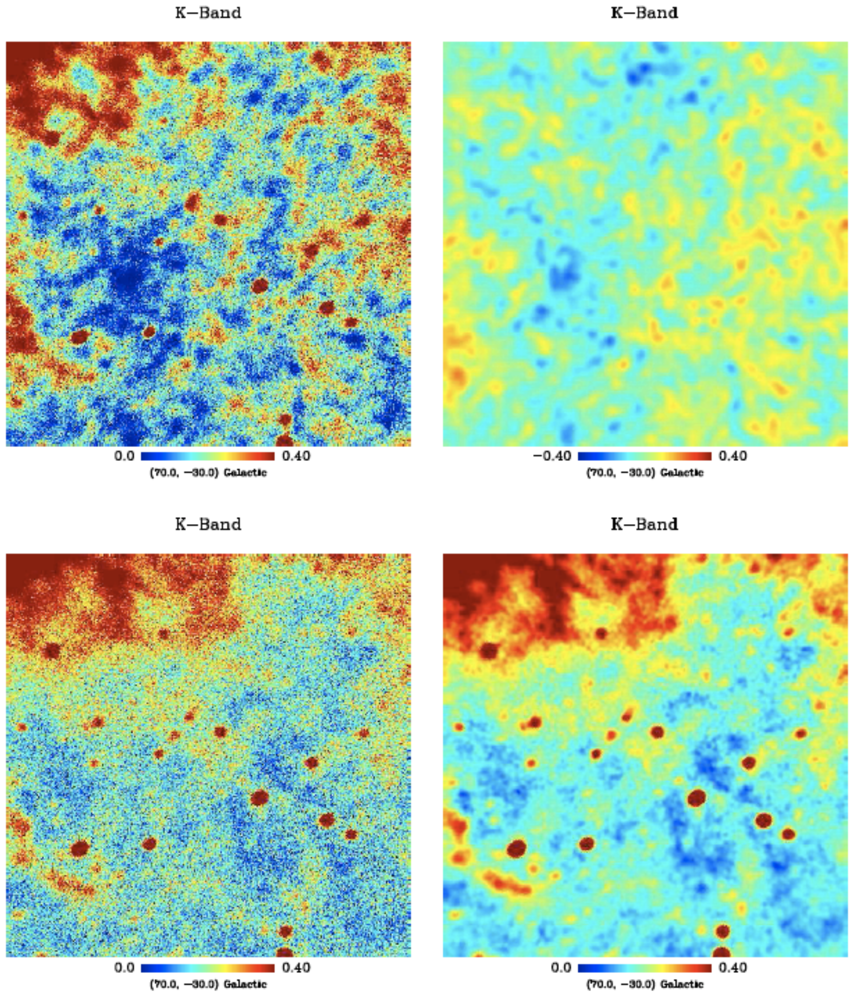

Foreground map

Filtered foreground map

Blind component separation - SMICA

Model in harmonic domain

$$x(\ell, m) = \mathbf{A} s(\ell, m) + n(\ell, m)$$

Spectral covariance matrices

$$\langle x x^t \rangle = \mathbf{A} \langle s s^t \rangle \mathbf{A}^{\mathbf{t}} + \langle n n^t \rangle$$

$$\begin{pmatrix} C_\ell^{x_1 x_1} & C_\ell^{x_1 x_2} & \cdots & C_\ell^{x_1 x_N} \\ C_\ell^{x_1 x_2} & C_\ell^{x_2 x_2} & \cdots & C_\ell^{x_2 x_N} \\ \vdots & \vdots & \ddots & \vdots \\ C_\ell^{x_1 x_N} & C_\ell^{x_2 x_N} & \cdots & C_\ell^{x_N x_N} \end{pmatrix}
\begin{pmatrix} a_1^{\mathrm{CMB}} & a_1^{\mathrm{dust}} & a_1^{\mathrm{sync}} & \cdots & a_1^{\mathrm{SZ}} \\ a_2^{\mathrm{CMB}} & a_2^{\mathrm{dust}} & a_2^{\mathrm{sync}} & \cdots & a_2^{\mathrm{SZ}} \\ \vdots & \vdots & \vdots & \ddots & \vdots \\ a_N^{\mathrm{CMB}} & a_N^{\mathrm{dust}} & a_N^{\mathrm{sync}} & \cdots & a_N^{\mathrm{SZ}} \end{pmatrix}
\begin{pmatrix} C_\ell^{\mathrm{CMB}} & 0 & 0 & \cdots & 0 \\ 0 & C_\ell^{\mathrm{dust}} & X_\ell & \cdots & 0 \\ 0 & X_\ell & C_\ell^{\mathrm{sync}} & \cdots & 0 \\ \vdots & \vdots & \vdots & \ddots & \vdots \\ 0 & 0 & 0 & \cdots & C_\ell^{\mathrm{SZ}} \end{pmatrix}
\begin{pmatrix} C_\ell^{n_1 n_1} & 0 & \cdots & 0 \\ 0 & C_\ell^{n_2 n_2} & \cdots & 0 \\ \vdots & \vdots & \ddots & \vdots \\ 0 & 0 & \cdots & C_\ell^{n_N n_N} \end{pmatrix}$$

Blind component separation - SMICA

$$\mathrm{R}_x(\ell) = \mathrm{A}\,\mathrm{R}_s(\ell)\,\mathrm{A}^t + \mathrm{R}_n(\ell)$$

$$\begin{pmatrix} C_\ell^{x_1x_1} & C_\ell^{x_1x_2} & \dots & C_\ell^{x_1x_N} \\ C_\ell^{x_1x_2} & C_\ell^{x_2x_2} & \dots & C_\ell^{x_2x_N} \\ \vdots & \vdots & \ddots & \vdots \\ C_\ell^{x_1x_N} & C_\ell^{x_2x_N} & \dots & C_\ell^{x_Nx_N} \end{pmatrix}$$

$$\widehat{C}_\ell^{x_ix_j} = \frac{1}{2\ell+1}\sum_{m=-\ell}^{\ell} x_{i,\ell m}\,\bar{x}_{j,\ell m}$$

OBSERVATIONS

$$\begin{pmatrix} a_1^{\mathrm{CMB}} & a_1^{\mathrm{dust}} & a_1^{\mathrm{sync}} & \dots & a_1^{\mathrm{SZ}} \\ a_2^{\mathrm{CMB}} & a_2^{\mathrm{dust}} & a_2^{\mathrm{sync}} & \dots & a_2^{\mathrm{SZ}} \\ \vdots & \vdots & \vdots & \ddots & \vdots \\ a_N^{\mathrm{CMB}} & a_N^{\mathrm{dust}} & a_N^{\mathrm{sync}} & \dots & a_N^{\mathrm{SZ}} \end{pmatrix}$$

$$\begin{pmatrix} C_\ell^{\mathrm{CMB}} & 0 & 0 & \dots & 0 \\ 0 & C_\ell^{\mathrm{dust}} & X_\ell & \dots & 0 \\ 0 & X_\ell & C_\ell^{\mathrm{sync}} & \dots & 0 \\ \vdots & \vdots & \vdots & \ddots & \vdots \\ 0 & 0 & 0 & \dots & C_\ell^{\mathrm{SZ}} \end{pmatrix}$$

$$\begin{pmatrix} C_\ell^{n_1n_1} & 0 & \dots & 0 \\ 0 & C_\ell^{n_2n_2} & \dots & 0 \\ \vdots & \vdots & \ddots & \vdots \\ 0 & 0 & \dots & C_\ell^{n_Nn_N} \end{pmatrix}$$

MODEL

SMICA is a *multi-component* maximum likelihood spectral estimation method

MODEL FITTING method

estimate the parameters of a model of CMB and foreground multivariate spectra

Blind component separation - SMICA

$$\sum_l w_l \left[\mathrm{tr}(\widehat{\mathbf{R}}_x \mathbf{R}_x^{-1}) - \log\det(\widehat{\mathbf{R}}_x \mathbf{R}_x^{-1}) \right]$$

minimise the mismatch between

$\mathsf{R}_x(\ell)$ and $\mathsf{A}\,\mathsf{R}_s(\ell)\,\mathsf{A}^t + \mathsf{R}_n(\ell)$

estimated spectral covariance of detector maps

modelled spectral covariance of detector maps

Planck CMB map with SMICA

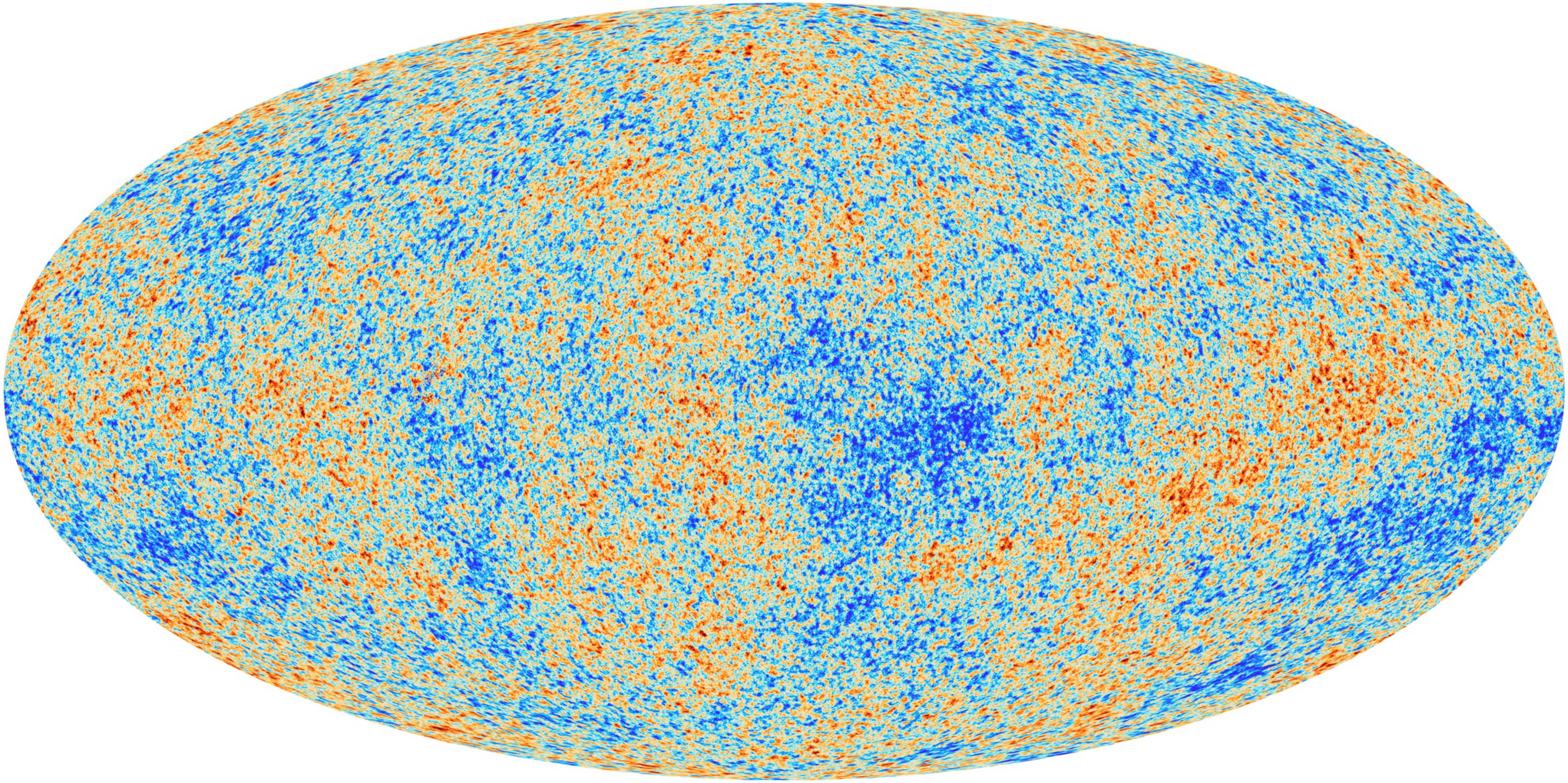

Key ingredients for it to work ?

- Many frequency channels (more than the dimension of the signal subspace at the level of the noise)
- Many independent data point for statistics

Outline

Astrophysical foreground emission

Basics of foreground cleaning

Component separation methods

➡ Forecasting and validation

Summary

Forecasting using simulations

1) Sky Model

Primordial B

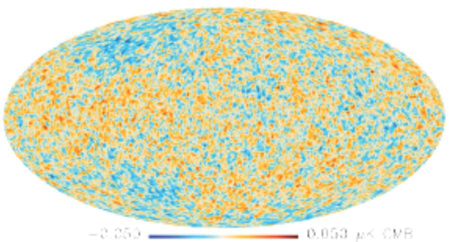

Lensing B

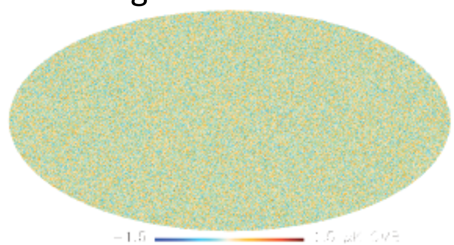

Synchrotron B at 60 GHz

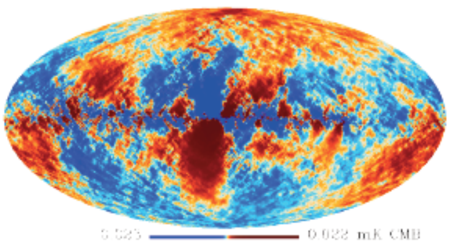

Dust B at 600 GHz

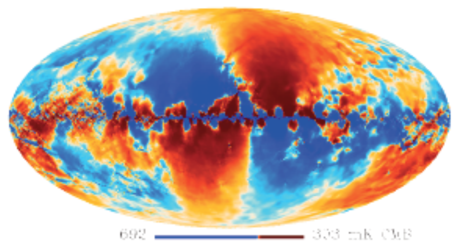

2) Frequency channels

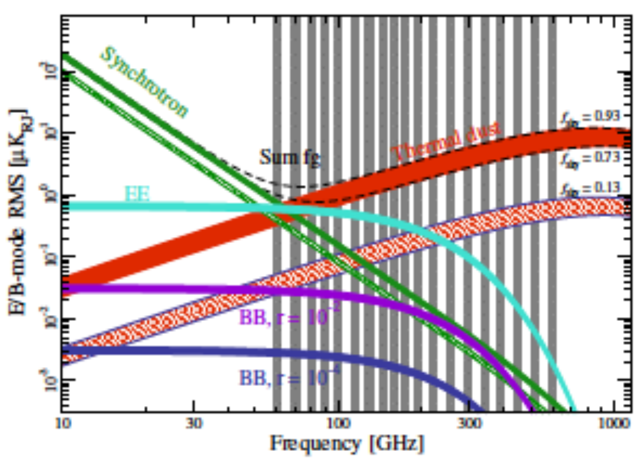

3) Analyse fake observations

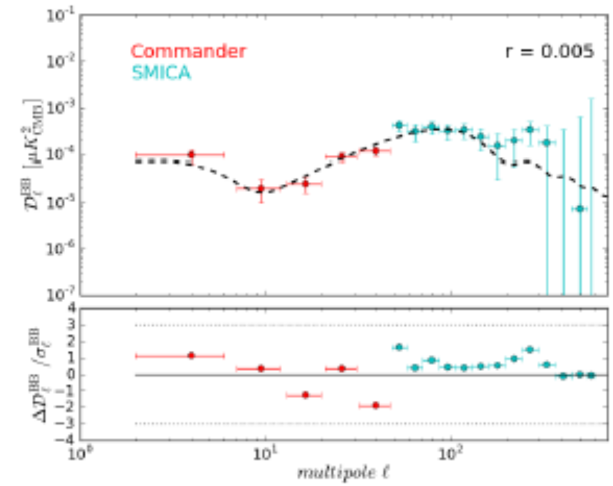

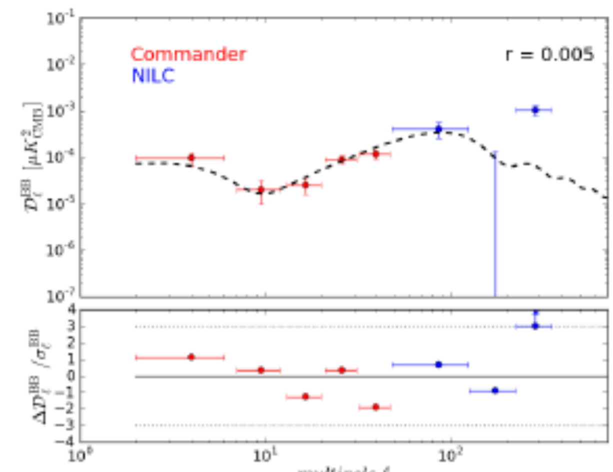

The BICEP2 "detection"

Ade et al., PRL 112, 24, id.241101 arXiv:1403.3985

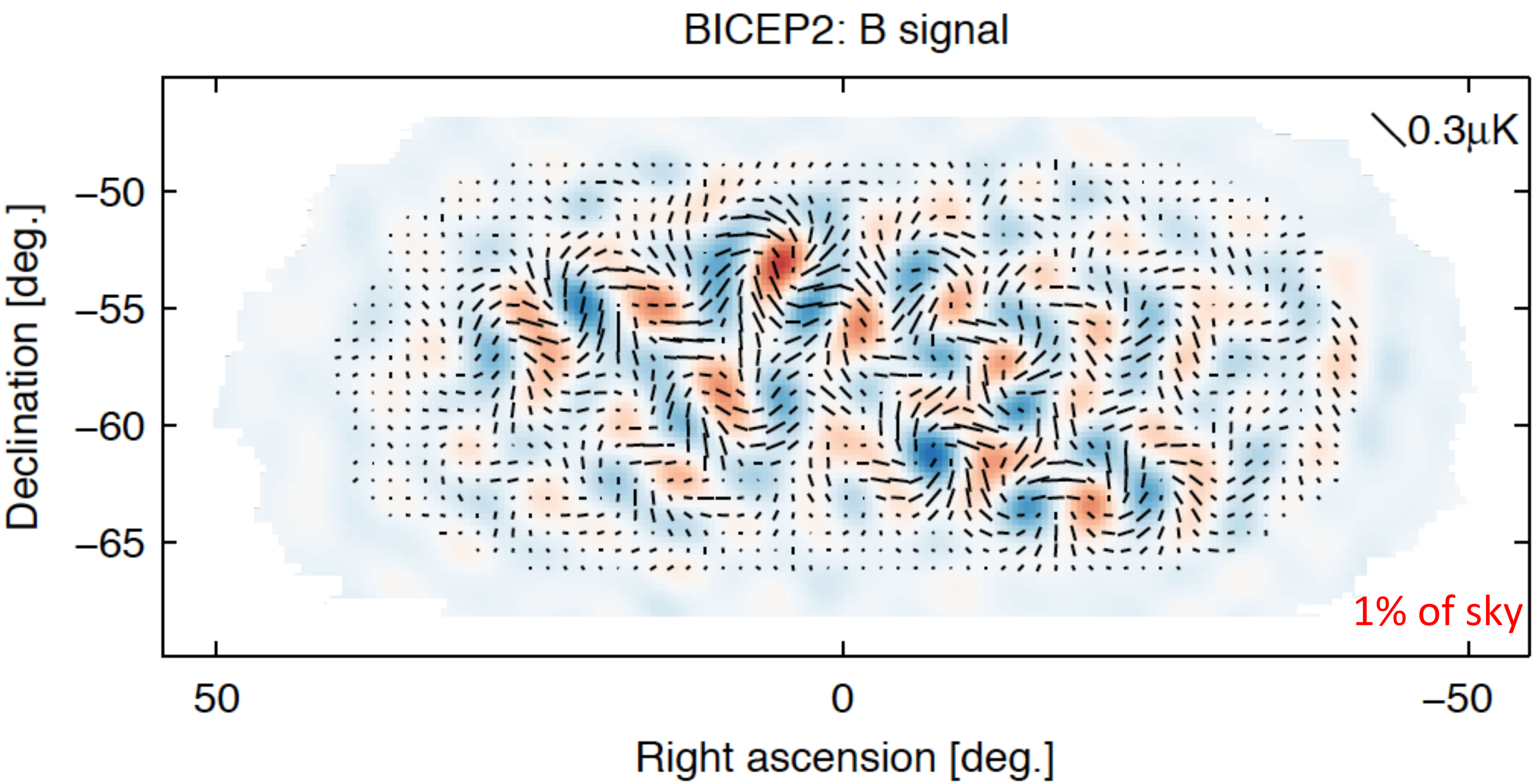

Amplitude of signal = about 0.1 μK

The BICEP2 "detection"

Ade et al., PRL 112, 24, id.241101 arXiv:1403.3985

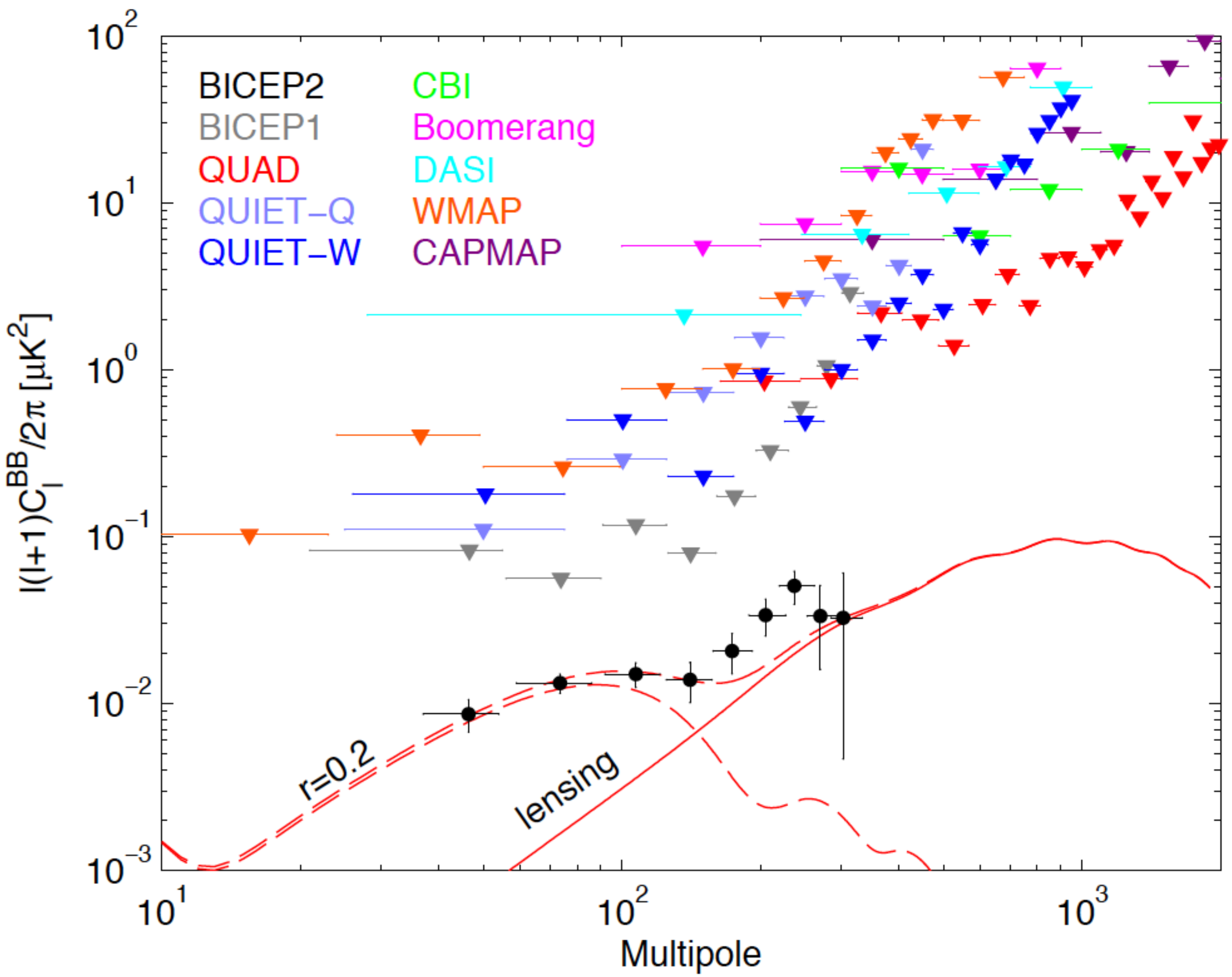

Validation on simulations (Planck case)

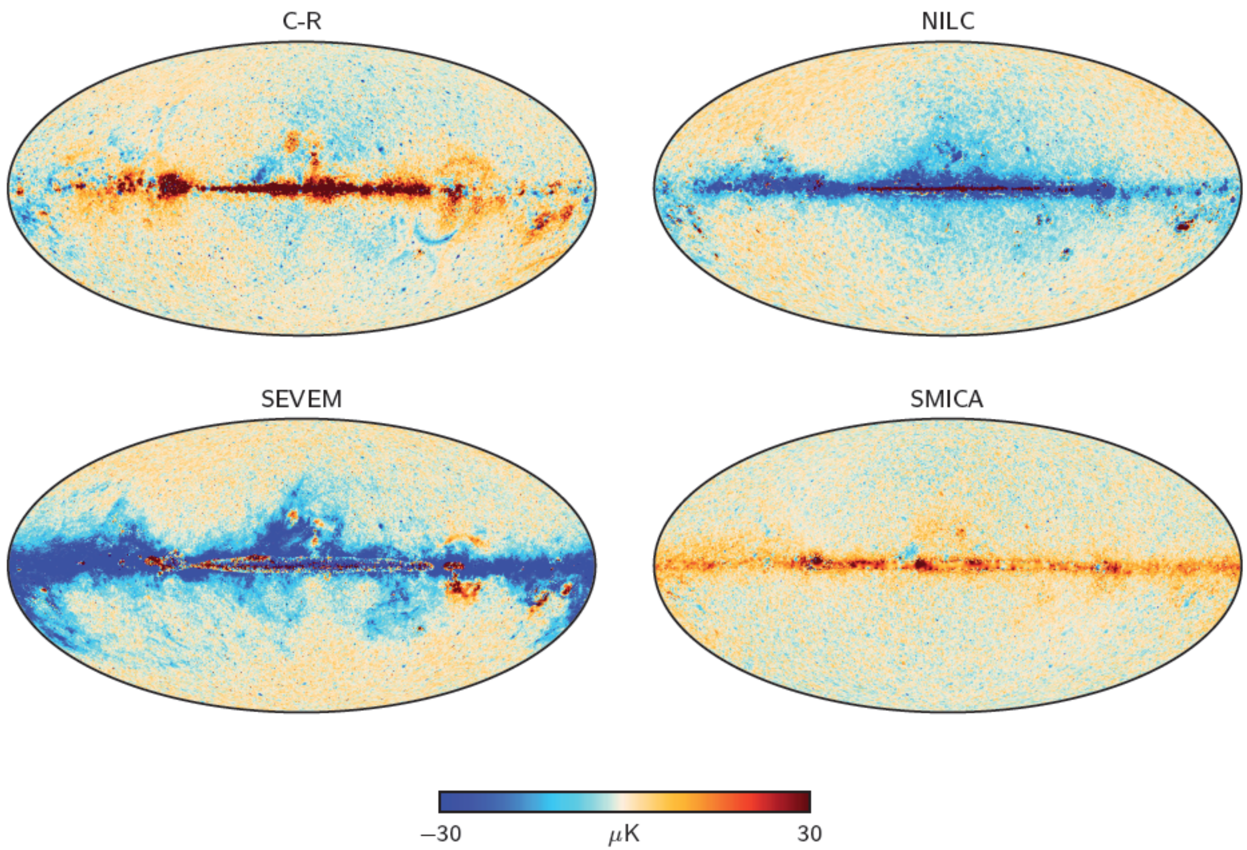

- Use FFP6 to illustrate the level of residuals expected from the component separation
- Maps have been downgraded to N_{side} = 128 to show large scale features

Obvious caveat: are the simulations representative ?

Validation by comparison

Compare maps

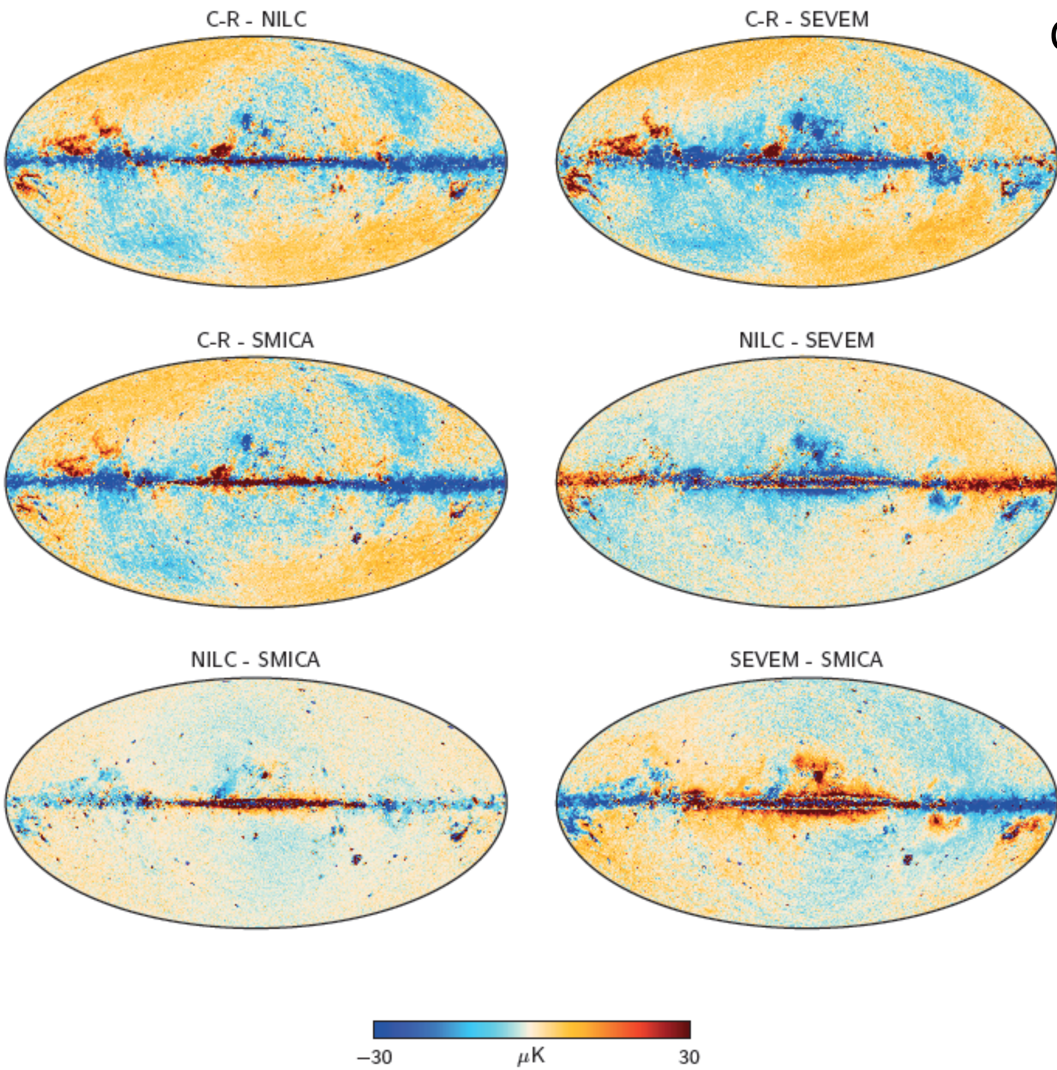

Fig. 6: Pairwise differences between foreground-cleaned CMB maps. All maps have been downgraded to a HEALPix resolution of $N_{\mathrm{side}} = 128$ to show the large-scale differences. The line-like discontinuities in the differences involving SEVEM is due to the two different regions used in this algorithm to clean the sky (see Appendix C for details).

Compare spectra

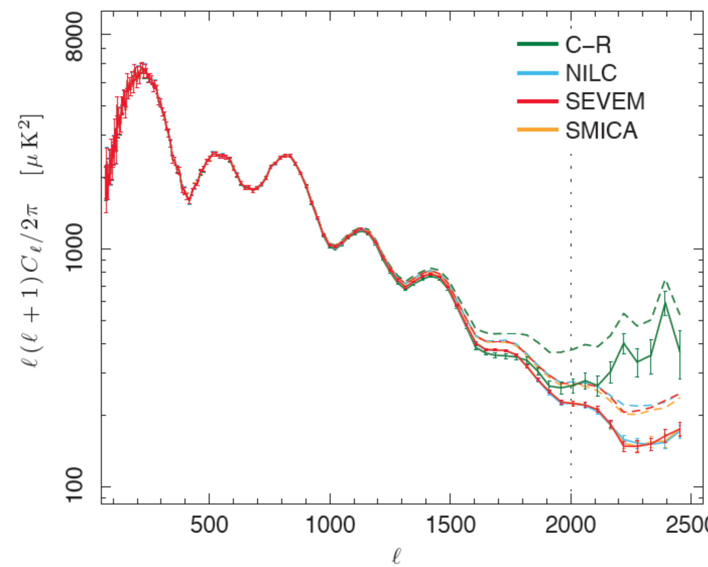

Fig. 10: Estimates of the CMB power spectra from the foreground-cleaned maps, computed by XFaster. The solid lines show the spectra after subtracting the best-fit model of residual foregrounds. The vertical dotted line shows the maximum multipole ($\ell = 2000$) used in the likelihood for fitting the foreground model and cosmological parameters (see Sect. 6.2.2 for further details). The dashed lines show the spectra before residual foreground subtraction.

Validation using analysis masks

Compare results obtained using different sky regions

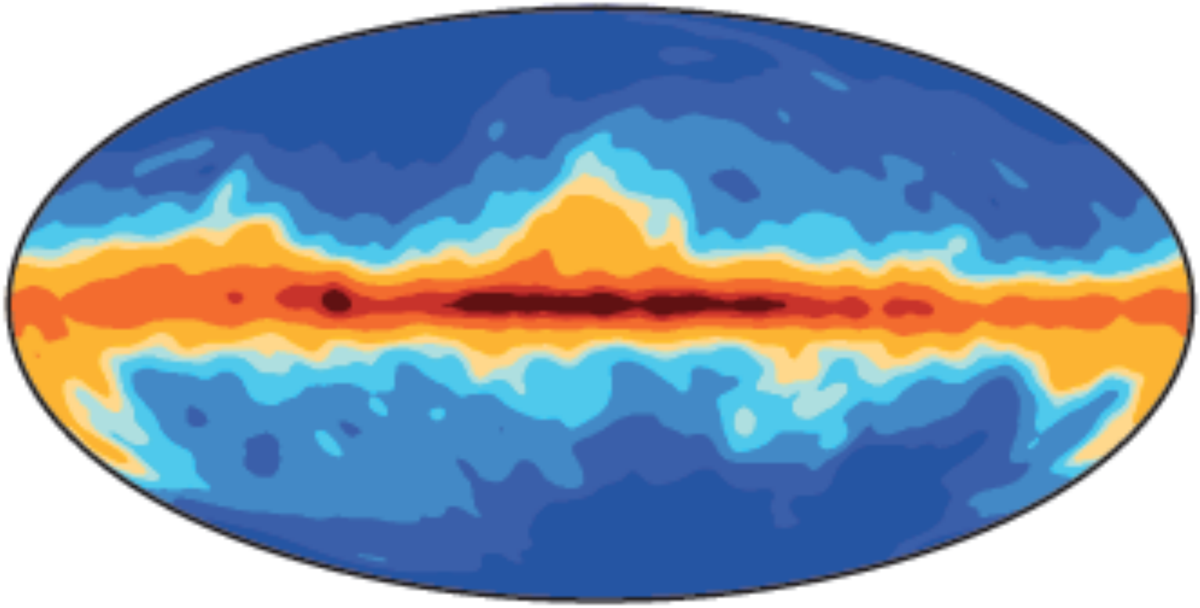

Fig. 2: Combined Galactic (CG) emission masks for the *Planck* data, corresponding to sky fractions of 20, 40, 60, 70, 75, 80, 90, 97, and 99 %. The masks are named CG20, etc.

Summary

- Confusion from foreground emission will be one of the major challenges for future CMB observations
- CMB B-modes will have to be detected below foreground emission that dominates by 2-3 orders of magnitude
- This is challenging, but with sensitive observations in many frequency channels, and with good angular resolution, there is good hope of success.
- This requires an ambitious space mission. Optimizing this space mission concept within practical constraints is the task at hand !

Thanks to colleagues who worked for many years to develop this field, some of whom are present in this meeting!